Molecular Dynamics Modeling of Chloride Binding to the Surfaces of Calcium Hydroxide, Hydrated Calcium Aluminate, and Calcium Silicate Phases

Andrey G. Kalinichev* and R. James Kirkpatrick

Department of Geology and Center for Advanced Cement-Based Materials, University of Illinois at Urbana-Champaign, 1301 West Green Street, Urbana, Illinois 61801

Received July 31, 2001. Revised Manuscript Received June 3, 2002

Molecular dynamics computer simulations are performed to study the structure and dynamical behavior of chloride and associated cations at the interfaces between aqueous solutions and portlandite ($Ca(OH)_2$), Friedel's salt ($[Ca_2Al(OH)_6]Cl{\cdot}2H_2O$), tobermorite ($Ca_5Si_6O_{16}(OH)_2$), and ettringite ($Ca_6[Al(OH)_6]_2[SO_4]_3{\cdot}26H_2O$). These phases are important in calcium silicate and calcium aluminate cements and are models of important poorly crystalline cement phases. They are also representative of many hydrous hydroxide, aluminate, and silicate materials stable near room temperature and pressure. The MD simulations use a recently developed semiempirical force field and take into account the flexibility of surface OH groups and allow for energy and momentum transfer between the solid and solution to effectively simulate the sorption. The principal focus is on the structure at and near the solution/solid interfaces and on the molecular mechanisms of adsorption of aqueous Cl^-, Na^+, and Cs^+ ions on a neutral portlandite surface and comparison to the Cl^- sorption behavior on the positively charged surface of Friedel's salt. Power spectra of molecular motions for bulk and surface species, diffusion coefficients for Cl^-, Na^+, and Cs^+ ions in different surface-related environments, and mean residence times on surface sites are calculated. Relative to the diffusion coefficients in bulk solution, those of Cl^- in an inner-sphere surface complex are reduced about an order of magnitude, those in outer-sphere complexes are reduced less, and for both types the coeffcients are reduced more for Friedel's salt than for portlandite. No Cl^- adsorption was observed on tobermotite, and little, on ettringite. The simulation results are in good qualitative agreement with experimental sorption and ^{35}Cl NMR studies. The MD results provide further confirmation that chloride binding on C−S−H, which is the most abundant phase in many cements, can be thought of as due to sorption on surface sites similar to those on portlandite.

Introduction

The interaction of ionic species and water molecules with the surfaces of oxide and hydroxide materials is central to understanding the chemical behavior of many environmentally and technologically important solid/water systems and has been the focus of numerous sorption and spectroscopic studies.[1] Because of the difficulty of studying these interactions in situ, however, many molecular scale aspects of these interactions remain poorly understood.[2] Sorption can be especially difficult to study because the lifetimes of the surface configurations are often short and the surface environments can be changed significantly by, for example, drying. We present here the results of a molecular dynamics (MD) computer modeling study of the sorption of aqueous chloride ion and associated cations (Na^+, K^+, Cs^+) with the surfaces of calcium hydroxide (portlandite), hydrated calcium aluminate phases (ettringite and the Cl^--containing Ca_2Al layered double hydroxide, Friedel's salt), and the calcium silicate, tobermorite. The results provide significant insight into the controls exerted by the structure and composition of the solid phase on the structural environments of the surface-associated species, the structure of the solution near the interface, and the translational, librational, and vibrational dynamics of the surface species including effective diffusion coefficients and approximate surface site residence times.

The phases studied are representative of those typically present in calcium silicate and calcium aluminate based cement systems,[3] but the approach is likely to be useful for many solution/solid interfaces. In particular, Friedel's salt, $[Ca_2Al(OH)_6]Cl{\cdot}2H_2O$, also known as hydrocalumite, is structurally one of the best understood of the layered double hydroxides (LDHs) and can serve as a model for other less ordered LDH phases. These compounds are receiving rapidly increasing attention for a wide variety of applications in catalysis, environmental remediation, and medicine.[4−6]

* Corresponding author. E-mail: kalinich@uiuc.edu.

(1) Sparks, D. L., Grundl, T. J., Eds. *Mineral-Water Interfacial Reactions*; ACS Symposium Series 715; American Chemical Society: Washington, DC, 1998.

(2) Brown, G. E. *Science* **2001**, *294*, 67.

(3) Taylor, H. F. W. *Cement Chemistry*, 2nd ed.; Thomas Telford Publishing: London, 1997.

10.1021/cm0107070 CCC: $22.00
Published on Web 07/23/2002

Our principal focus here is on chloride, because its migration through cement paste is a key process in the degradation of concrete structures due to both structural changes in the paste and loss of passivation of the oxide film on the steel reinforcement and its subsequent oxidation and expansion.[7−9] Recent sorption isotherm and ^{35}Cl NMR Cl^- relaxation studies have substantially improved understanding of the structural and compositional controls of Cl^- binding to the surfaces of these and similar phases,[10,11] and the modeling presented here builds on this understanding. We discuss the alkali cations in less detail.

Molecular modeling methods are increasingly being used to study local structural environments and dynamical processes of ions and water in the interlayers of clays, other layered-structure phases, and the pores of zeolites.[12−18] Because the behavior of these systems is also dominated by Coulombic and hydrogen bonding interactions, it is in many ways comparable to the molecular dynamics modeling of surface-binding presented in this paper.

Simulation Methods and Structural Results

Molecular modeling of solid/solution interfaces can be particularly complicated for many oxide and hydroxide phases, such as clays and the cement phases studied here, because they often have complex crystal structures, low symmetry, large unit cells, and variable composition. Moreover, they frequently occur as micron to submicron size particles, and their structure is often incompletely or poorly characterized. We approach these problems by starting our simulation efforts from the structures of relatively well-understood crystalline model phases and applying the recently developed CLAYFF force field to model all ion−ion and ion−water interactions.[19]

It is a common practice in many molecular modeling studies of the solid/solution interfaces to treat the atoms of the solid as fixed on a rigid lattice,[14−16] although sometimes allowing motions associated with swelling and lateral displacement of the lattice as a whole. This approach can save substantial amounts of computer time, because the degrees of freedom associated with the motion of individual atoms in the solid substrate are excluded from the calculations. Such models obey all fundamental mechanical conservation laws, but because of the immobility of the lattice atoms, the exchange of energy and momentum among the interacting atoms of the substrate and the surface solution species (inelastic interactions) is not possible. Thus, this approach introduces an a priori distortion into the atomistic description of the structural and dynamic behavior of surface species. The magnitude of this distortion and whether it can be safely neglected ultimately depend on the characteristic time scales of the different types of relevant atomic motions and the degree of mechanical coupling between them in the simulated systems. In particular, for the hydrated phases in our simulations, the characteristic time scales of vibrational and librational motions for surface OH groups are definitely comparable to those of similar motions of H_2O molecules and hydrated ions in the aqueous phase. Thus, accurate representation of the dynamics of such processes as hydrogen bonding, adsorption, surface hydration, and complexation can be inherently limited if the atoms of the substrate layer are all considered completely immobile. Surface diffusion rates of ions and water molecules can also be overestimated, and the structure of the aqueous layers at the interface can be distorted.

There are two possibilities to introduce the mobility and flexibility of the solid substrate in computer simulations of solid/solution interfaces. One can explicitly introduce a set of bonded interaction terms in addition to commonly used electrostatic and van der Waals terms of the force field. In this approach, bonds must be identified and evaluated for each possible interatomic coordination.[12,17] However, the application of such an approach to systems with complex and ill-defined bond structures can be problematic, because it leads to significant overparametrization of the force field, due to lack of the experimental data to constrain all the parameters necessary to describe bonded interactions.

The development of the CLAYFF force field used in our simulations was based on an alternative approach to the description of the metal−oxygen interactions associated with hydrated phases.[19] It incorporates these interactions as ionic (i.e., nonbonded), thus allowing the simulations of even complex disordered systems containing large numbers of atoms. CLAYFF allows for unrestricted exchange of momentum and energy among all species present in the crystal structure as well as in the aqueous phase. The specific methods and algorithms used for the development and validation of the force field are discussed in detail elsewhere.[19] Here we only briefly mention that the parameters of the CLAYFF force field are specifically optimized on the basis of the observed structures of simple oxides, hydroxides, and oxyhydroxides, with partial atomic charges derived from periodic DFT quantum calculations of these model compounds. The charges on oxygen and hydrogen atoms can vary because of their occurrence in water molecules, hydroxyl groups, and bridging sites and with nearest neighbor cation substitution. The force field accounts for charge delocalization due to cation substitution (e.g., Al for Si, or Ca for Al) such that charge is removed from the

(4) Cavani, F.; Trifiro, F.; Vaccari, A. *Catal. Today* **1991**, *11*, 173.
(5) Newman, S. P.; Jones, W. *New J. Chem.* **1998**, *22*, 105.
(6) Choy, J. H.; Kwak, S. Y.; Jeong, Y. J.; Park, J. S. *Angew. Chem., Int. Ed.* **2000**, *39*, 4041.
(7) Ramachandran, V. S. *Mater. Constr.* **1971**, *4*, 3.
(8) Beaudoin, J. J.; Ramachandran, V. S.; Feldman, R. F. *Cem. Concr. Res.* **1990**, *20*, 875.
(9) Garboczi, E. J.; Bentz, D. P. *Adv. Cem. Based Mater.* **1998**, *8*, 77.
(10) Yu, P.; Kirkpatrick, R. J. *Cem. Concr. Res.* **2001**, *31*, 1479.
(11) Kirkpatrick, R. J.; Yu, P.; Kalinichev, A. G. In *Calcium Hydroxide in Concrete*; Skalny, J., Ed.; American Ceramics Society: 2001; Materials Science of Concrete Special Volume, pp 77−92.
(12) Teppen, B. J.; Rasmussen, K.; Bertsch, P. M.; Miller, D. M.; Schafer, L. *J. Phys. Chem. B* **1997**, *101*, 1579.
(13) Aicken, A. M.; Bell, I. S.; Coveney, P. V.; Jones, W. *Adv. Mater.* **1997**, *9*, 496.
(14) Smith, D. E. *Langmuir* **1998**, *14*, 5959.
(15) Chang, F. R. C.; Skipper, N. T.; Sposito, G. *Langmuir* **1998**, *14*, 1201.
(16) Greathouse, J. A.; Refson, K.; Sposito, G. *J. Am. Chem. Soc.* **2000**, *122*, 11459.
(17) Bougeard, D.; Smirnov, K. S.; Geidel, E. *J. Phys. Chem. B* **2000**, *104*, 9210.
(18) Cygan, R. T. *Rev. Mineral. Geochem.* **2001**, *42*, 1.
(19) Cygan, R. T.; Liang, J.-J.; Kalinichev, A. G. Manuscript in preparation.

cationic center to neighboring oxygens depending on the local O-environment.

The force field parameters for aqueous cations and anions are largely incorporated from published intermolecular functions.[20−23] For water−water interactions we used the flexible version[24] of the simple point charge (SPC) interaction potential.[25] This potential is one of the most frequently used models of water and is capable of producing reliable results in molecular simulations of a wide range of aqueous phases.[26] For consistency, the Lennard-Jones terms centered on all types of O atoms in the CLAYFF force field were assumed to be equivalent to the SPC water oxygens, while those centered on the H atoms of OH groups were ignored. The harmonic potential of the hydroxide O−H stretching vibrations was also taken to be equivalent to that of the SPC H_2O model.[24] The harmonic terms describing the bond stretching and bond angle bending associated with water molecules, hydroxyls, and polyatomic anions are the only type of bonded interactions explicitly defined in the CLAYFF force field.[19]

The CLAYFF force field has already been used to successfully model the structures of oxide and hydroxide materials, the interactions of aqueous species with oxide and hydroxide surfaces, and the behavior of water and ionic species in the interlayers of layer-structure phases.[18,19,27−29] Moreover, recently simulated far-infrared spectra of LDH phases[30] demonstrate surprisingly good agreement between the observed and calculated band positions, although the force field was not specifically optimized to simulate either LDHs or vibrational frequencies.

The total potential interaction energy of the simulated system is calculated as a sum of an electrostatic term for all Coulomb interactions between partial atomic charges and a Lennard-Jones (12−6) term modeling the short-range van der Waals dispersive interactions:

$$U = \sum_{i,j}\left\{\frac{q_i q_j}{4\pi\epsilon_0 r_{ij}} + 4\epsilon_{ij}\left[\left(\frac{\sigma_{ij}}{r_{ij}}\right)^{12} - \left(\frac{\sigma_{ij}}{r_{ij}}\right)^{6}\right]\right\} \qquad (1)$$

where r_{ij} is the distance between atoms i and j, q_i and q_j are partial charges centered on these atoms, ϵ_{ij} and σ_{ij} are parameters of the Lennard-Jones interaction potential, and ϵ_0 is the dielectric permittivity of vacuum ($\epsilon_0 = 8.854\,19 \times 10^{-12}$ F/m). The Lennard-Jones parameters of unlike interactions were calculated according to the "arithmetic" combining rules:

$$\sigma_{ij} = \frac{\sigma_{ii} + \sigma_{jj}}{2}; \quad \epsilon_{ij} = \sqrt{\epsilon_{ii}\epsilon_{jj}} \qquad (2)$$

A "spline cut-off" method was used to treat the non-Coulomb interactions, and all long-range electrostatic interactions were treated using the Ewald summation method.[31]

Table 1. Crystallographic Lattice Parameters of Simulated Phases (the Second Row for Each Parameter Represents Available Experimental Values)

	portlandite[33,34]	Friedel's salt[35]	tobermorite[36]	ettringite[37]
a/Å	3.57	10.02	11.16	11.02
	3.59	9.979	11.16	11.26
b/Å	3.57	5.94	7.26	10.94
	3.59	5.751	7.30	11.26
c/Å	4.91	15.99	9.61	21.30
	4.91	16.320	9.57	21.46
α/deg	90.01	90.00	103.47	90.50
	90.00	90.00	101.08	90.00
β/deg	89.98	102.89	89.46	89.80
	90.00	104.53	92.83	90.00
γ/deg	120.01	90.00	90.13	119.80
	120.00	90.00	89.98	120.00
V/Å^3	54.3	927.6	757.8	2232.3
	54.82	906.64	763.87	2358.53

Molecular dynamics modeling was undertaken for four phases—portlandite (crystalline $Ca(OH)_2$), the Cl^--containing calcium−aluminum layered double hydroxide (Friedel's salt), ettringite, and tobermorite—and their interfaces with aqueous alkali−chloride solutions. These phases were chosen to be representative of the phases and types of surface sites present in calcium silicate and calcium aluminate cement systems,[3] but they are also representative of many oxide and hydroxide materials. Portlandite is present as a separate phase in cements. Tobermorite is a model for the calcium silicate hydrate phase (C−S−H in cement nomenclature), and structural models of C−S−H phases suggest that the more Ca-rich examples may expose surface sites similar to those of tobermorite and portlandite.[32] Friedel's salt is representative of the layer-structure calcium aluminate phases (AFm in cement nomenclature), and the behavior at its surface is unlikely to be greatly affected by the interlayer anions, because they are so far from the surface. Ettringite is a common, well-crystallized phase in some cements.

The structure of portlandite is well-known from the literature.[33,34] The simulation supercell contained 8 × 8 × 4 crystallographic unit cells of portlandite in the a, b, and c directions, respectively. Except for the 3-dimensional periodic boundary conditions[31] imposed on the supercell, we applied no additional symmetry constraints. The structure was treated as triclinic $P1$, and all cell parameters, a, b, c, α, β, and γ, were considered to be independent variables during the structure optimization that minimized the total energy of the system. The computed structure is in very good agreement with experimental data[33,34] (Table 1). This result was expected, because the portlandite structure was used to

(20) Dang, L. X. *J. Am. Chem. Soc.* **1995**, *117*, 6954.
(21) Lee, S. H.; Rasaiah, J. C. *J. Chem. Phys.* **1994**, *101*, 6964.
(22) Cannon, W. R.; Pettitt, B. M.; McCammon, J. A. *J. Phys. Chem.* **1994**, *98*, 6225.
(23) The full set of force field parameters used is listed in Table 1s of Supporting Information.
(24) Teleman, O.; Jönsson, B.; Engström, S. *Mol. Phys.* **1987**, *60*, 193.
(25) Berendsen, H. J. C.; Postma, J. P. M.; van Gunsteren, W. F.; Hermans, J. In *Intermolecular Forces*; Pullman, B., Ed.; Riedel: Dordrecht, 1981; p 331.
(26) Kalinichev, A. G. *Rev. Mineral. Geochem.* **2001**, *42*, 83.
(27) Kalinichev, A. G.; Kirkpatrick, R. J.; Cygan, R. T. *Am. Mineral.* **2000**, *85*, 1046.
(28) Wang, J.; Kalinichev, A. G.; Kirkpatrick, R. J.; Hou, X. *Chem. Mater.* **2001**, *13*, 145.
(29) Hou, X.; Kalinichev, A. G.; Kirkpatrick, R. J. *Chem. Mater.* **2002**, *14*, 2078.
(30) Wang, J.; Kalinichev, A. G.; Amonette, J.; Kirkpatrick, R. J. *Am. Mineral.* (in press).
(31) Allen, M. P.; Tildesley, D. J. *Computer Simulation of Liquids*; Oxford University Press: New York, 1987.
(32) Cong, X.; Kirkpatrick, R. J. *Adv. Cem. Based Mater.* **1996**, *3*, 144.
(33) Petch, H. E. *Acta Crystallogr.* **1961**, *14*, 950.
(34) Desgranges, L.; Grebille, D.; Calvarin, G.; Chevrier, G.; Floquet, N.; Niepce, J. C. *Acta Crystallogr.* **1993**, *B49*, 812.

Table 2. Molecular Dynamics Simulation Details

MD run no.	1	2	3	4	5	6	7
system	portlandite	portlandite	Friedel's salt	Friedel's salt	tobermorite	ettringite	ettringite
crystal supercell size (unit cells)	8 × 8 × 4	8 × 8 × 4	2 × 4 × 2	2 × 4 × 2	2 × 4 × 2	2 × 2 × 1	2 × 2 × 1
supercell size/Å^3 (*a*, *b*, *c* dimensions)	29 × 29 × 58	29 × 29 × 58	20 × 23 × 60	20 × 23 × 60	23 × 29 × 60	22 × 22 × 56	22 × 22 × 56
thickness of solution layer/Å	~38	~38	~27	~27	~40	~30	~30
total no. of atoms	1288 + 875 H_2O + 4 NaCl	1288 + 875 H_2O + 4 CsCl	1408 + 387 H_2O	1408 + 387 H_2O + 2 NaCl	992 + 882 H_2O + 4 KCl	1374 + 425 H_2O + 4 NaCl	1374 + 425 H_2O + 4 NaCl
simulation length/ps	80 + 80	120 + 120	100 + 100	100 + 100	100 + 100	100 + 100	100 + 100
trajectory sampled every/ps	0.01	0.01	0.01	0.01	0.01	0.01	0.01
analyzed equil config	8000	12000	10000	10000	10000	10000	10000

parametrize the CLAYFF force field.[19] The initial structure of Friedel's salt, $[Ca_2Al(OH)_6]Cl{\cdot}2H_2O$, was taken from the single-crystal X-ray diffraction data.[35,38] The simulation supercell contained 2 × 4 × 2 crystallographic unit cells in the *a*, *b*, and *c* directions, respectively. Again, the original symmetry (monoclinic *C*2/*c*) was replaced by triclinic *P*1, and all cell parameters, *a*, *b*, *c*, α, *β*, and *γ*, were treated as independent variables during the crystal structure optimization. The agreement with experimental data is very good (Table 1), given that this structure was not used for the original force field parametrization. The simulation supercell of tobermorite contained 2 × 4 × 2 crystallographic unit cells of the so-called "tobermorite 9 Å", $Ca_5Si_6O_{16}(OH)_2$.[36,38] For ettringite,[37,38] $Ca_6[Al(OH)_6]_2[SO_4]_3{\cdot}26H_2O$, the simulation supercell contained 2 × 2 × 1 unit cells in the *a*, *b*, and *c* directions, respectively. For both tobermorite and ettringite, the experimentally undetermined positions of H atoms in hydroxyl groups and water molecules in the crystal structure were initially assigned assuming the existence of a stable network of hydrogen bonds with neighboring atoms. The positions of all atoms and the crystallographic unit cell parameters were then optimized using the algorithm described above. The resulting structures are in surprisingly good agreement with the observed structures, which were not used in the CLAYFF parametrization (Table 1).

To simulate the interfaces of the solid phases with aqueous solutions, the optimized layered structures of portlandite, Friedel's salt, and tobermorite were cleaved parallel to the layering ((001) crystallographic plane), whereas the columnar ettringite structure was cleaved parallel to the (100) plane. This procedure exposes only OH groups and O atoms on the surfaces, as is normally the case for such materials in contact with water.[1,2] The surfaces created were brought into contact with a layer of aqueous solution 27−40 Å thick. Periodic boundary conditions[31] were then applied in all three dimensions to produce models of the interfaces formed by the solid layers interspersed with layers of aqueous solutions (Table 2 and Figure 1).[38] In all cases, the thickness of the solution layer was sufficiently large to effectively exclude direct interactions between two different solution/solid interfaces created because of the periodicity of the system. The number of H_2O molecules in this layer was chosen to reproduce the density of the bulk aqueous solution under ambient conditions (~1 g/cm^3). For all runs except for those with Friedel's salt, there were initially four Cl^- and four cations in the water layer, which corresponds to a solution concentration range of 0.25−0.4 molal. These concentrations are within and near the upper limit of concentrations found in the pore solutions of cements.[3,7−11] For comparison, we also performed MD simulations of a bulk NaCl aqueous solution with the same concentration and with the same set of interaction parameters.

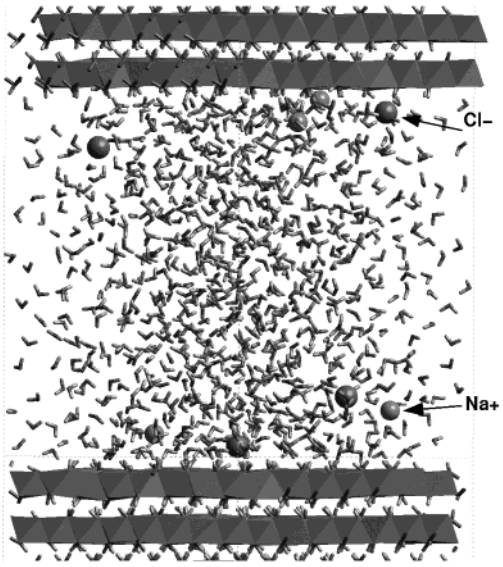

Figure 1. Snapshot of the simulation cell for portlandite and a 0.25*m* NaCl aqueous solution illustrating a typical simulation cell. Blue octahedra are Ca; red cylinders are O; gray cylinders are H; green balls are Cl^- ions; and pink balls are Na^+ ions. The thickness of the solution layer is ~40 Å. Only part of the solid layer is shown.

Molecular dynamics trajectories for all systems were generated using the Cerius^2 molecular modeling package.[39] A time step of 0.001 ps was used, and each equilibrium MD trajectory extended to 80−120 ps (typically 100 ps). To ensure the thermodynamic equilibrium in each run, the convergence of total energy and its components, as well temperature, pressure, and radial distribution functions for solution species, were carefully monitored during a pre-equilibration period of about 100 ps before the equilibrium trajectory was recorded for further statistical analysis. The Hoover *NVT*-ensemble MD algorithm[40] was employed for all simulations, and the temperature was set equal to 298

(35) Terzis, A.; Filippakis, S.; Kuzel, H. J.; Burzlaff, H. *Z. Kristallogr.* **1987**, *181*, 29.
(36) Merlino, S.; Bonaccorsi, S.; Armbruster, T. *Am. Mineral.* **1999**, *84*, 1613.
(37) Moore, A. E.; Taylor, H. F. W. *Acta Crystallogr.* **1970**, *B26*, 386.
(38) Full-color snapshots of representative portions of the simulated structures of Friedel's salt, tobermorite, and ettringite are shown in Figures 1s, 2s, and 3s of Supporting Information.
(39) Molecular Simulations Inc. *Cerius2−4.0 User Guide. Forcefield-Based Simulations*; MSI: San Diego, CA, 1999.
(40) Hoover, W. H. *Phys. Rev. A* **1985**, *31*, 1695.

Table 3. Adsorption of Cl^- Ions on the Surface of Model Cement Phases

system (MD run no.)	portlandite (1)	portlandite (2)	Friedel's salt (3)	Friedel's salt (4)	tobermorite (5)	ettringite (6)	ettringite (7)
fraction of surface-bound Cl^-/%	65	65	95	85	0	0	20
fraction of surface-bound counterions/%	85	60	0	0	25	25	25
Cl^- surface residence time/ps	~20	~20	~50	~50	N/A[a]	N/A	~50

[a] N/A = not applicable.

K. At the beginning of the pre-equilibration stage for each system, all ions in the aqueous phase were positioned at distances not less than 8−10 Å (~3 molecular diameters of H_2O) from the solid surface, and their dynamic evolution and possible adsorption to the surface were carefully monitored in the simulations. Typically, those atoms that become associated with the interface move to it during the pre-equilibration stage. However, the quantitative estimates for diffusion coefficients, adsorption site residence times, power spectra of atomic motions, and structural environments of adsorbed species were obtained only from the analysis of the equilibrium stage of each MD trajectory. Details of the simulation runs are given in Table 2.

The two simulations for portlandite (runs 1 and 2 in Table 2) differed largely in the cations present in the solution (Na^+ or Cs^+) to charge balance Cl^-, which is the main object of the present study. For Friedel's salt, Cl^- ions are naturally present at the cleaved surface, since they are part of the crystal structure.[35] In one MD simulation for this material (run 3), these were the only chloride ions present at the solution/solid interface, but in the other simulation (run 4), some NaCl was added to the solution. In both cases, all ions were initially positioned away from the surface before pre-equilibration. Similarly, for ettringite, sulfate ions are naturally present at the cleaved surface, and the two MD simulations for it (runs 6 and 7 in Table 2) differed in their starting configurations as follows. In run 6, only Na^+ and Cl^- ions were positioned away from the surface before pre-equilibration, whereas SO_4^{2-} ions remained on their natural positions in the crystal structure. In run 7, the surface SO_4^{2-} ions were also initially moved deep into the solution phase before pre-equilibration.

Every 10th time step during the equilibrium stage of the simulations, all atomic coordinates and velocities were recorded for further statistical analysis. Thus, for each model system we were able to analyze an equilibrium dynamic trajectory consisting of 8000−12000 atomic configurations with a time resolution of 10^{-14} s. This resolution is sufficient to construct power spectra of translational, librational, and low-frequency vibrational atomic motions by Fourier transformation of the corresponding velocity autocorrelation functions.[31,41]

Surface Adsorption of Ions and the Structure of the Solid/Solution Interface

In our analysis of the ionic adsorption, we qualitatively distinguish three types of species in the aqueous phase (e.g., Figure 1): (1) inner-sphere surface complexes, that is, ions directly coordinated by atoms in the solid surface; (2) outer-sphere surface complexes, that is, ions separated from the surface by one molecular layer of water; and (3) ions in the diffuse layer, or in the bulk solution, that is, the ones separated from the surface by more than one molecular layer of water. The structural and dynamic properties of the last type of ions are also affected by the presence of the surface, but for simplicity, we classify them all as one "bulk" type. The number of ions present in the simulations was not sufficient to effectively probe the macroscopic behavior of the diffuse (Gouy) layer near the surface, the size of which is estimated to be comparable to the thickness of the entire aqueous layer in our simulations. Additionally, many ions change their positions with respect to the surface and hence their classification in the procedure described above during the equilibrium stage of the simulation. Therefore, the dynamics and hydration structure for different types of surface ions can only be analyzed on a semiquantitative basis. However, the characteristic relaxation time of the atomic velocity autocorrelation functions for all species was always at least an order magnitude shorter than the typical residence time of the surface species (Table 3), justifying the classification above and the following analysis.

The simulations show significant differences in the interaction of Cl^- with the surfaces of the solid phases studied. For portlandite, 65% of the Cl^- occurred in the surface, and for Friedel's salt, 85−95% (Table 3, runs 1−4). For ettringite, only one Cl^- (20%) was able to occupy a surface site belonging to sulfate in run 7, which started with the chloride and sulfate in the bulk solution. However, Cl^- could not displace surface sulfate in the run with all the sulfates initially on the surface (run 6), demonstrating the weak Cl^- exchange capability of this material. For tobermorite, no surface-bound Cl^- ions were observed on the time scale of our simulations. This result confirms the low Cl^- sorption capacity of this phase.[10,11] Cl^- sorption at similar sites on the C−S−H phase should be as low or lower, because the tobermoite model used in this study contained a full set of Si−OH surface sites, whereas previous studies have shown that at the Ca/Si ratios and pH values relevant to most cements the Si−O sites are deprotonated.[32,42] The negative charge of the bare surface O atoms should repel the Cl^- even more strongly. For portlandite, tobermorite, and ettringite, the cations were also attracted to the solid surfaces. The structural environments and dynamical behavior of the surface-sorbed species are different on different phases, and the MD results provide significant insight into how the structures and compositions control these features.

Surface Environments and Surface Influence on Cl^- Diffusion. Interaction of Cl^- with the portlandite,

(41) McQuarrie, D. A. *Statistical mechanics*; Harper & Row Publishers: 1976; pp 553−561.

(42) Yu, P.; Kirkpatrick, R. J.; Poe, B.; McMillan, P. F.; Cong, X. D. *J. Am. Ceram. Soc.* **1999**, *82*, 742.

Table 4. Cl^- Diffusion Coefficients (cm^2/s) under Ambient Conditions[a]

system (MD run no.)	portlandite (1)	portlandite (2)	Friedel's salt (3)	Friedel's salt (4)	ettringite (7)
interlayer	N/A[b]	N/A	$\ll 10^{-7}$	$\ll 10^{-7}$	$\ll 10^{-7}$
surface (inner sphere)	3.6×10^{-6}	3.8×10^{-6}	1.6×10^{-6}	1.6×10^{-6}	2.0×10^{-6}
surface (outer sphere)	1.5×10^{-5}	1.4×10^{-5}	8.0×10^{-6}	7.2×10^{-6}	3.8×10^{-6}
total surface-bound	1.1×10^{-5}	0.92×10^{-5}	2.3×10^{-6}	1.9×10^{-6}	3.5×10^{-6}

[a] Bulk NaCl solution: 2.3×10^{-5}. [b] N/A = not applicable.

Friedel's salt, and ettringite surfaces significantly reduces their rates of diffusion, and inner-sphere Cl^- is affected more than outer-sphere Cl^- (Table 4). The diffusion coefficients of all species were calculated through the mean-square displacement formula.[31,39] Statistical errors in the calculated diffusion coefficients are roughly 10−15%. For portlandite (runs 1 and 2), the inner-sphere Cl^- diffusion rate is reduced a factor of 6 relative to that of bulk solution, whereas, for outer-sphere Cl^-, this reduction is only about a factor of 1.5. Portlandite has no permanent structural charge to attract ions, and the simulations suggest that hydrogen bonding to the Cl^-, the mobility of the surface OH, and the flexibility of the surface Ca−O−H bond angles play important roles in creating favorable local electrostatic environments for the adsorption. As shown in Figure 2a, the surface OH groups bend toward the surface Cl^- to allow H-bonding. Typically, the inner-sphere surface Cl^- ions are coordinated by three surface OH groups, and they can be located over either the tetrahedral vacancy or the Ca octahedron. These hydrogen bonds complete a nearest neighbor coordination shell very similar to the Cl^- hydration shell in a bulk solution. In contrast, the adsorbed cations are stabilized by the surface OH groups bending away from the ion, thus exposing the cations to the negatively charged oxygens of the surface hydroxyls (Figure 2a).

Friedel's salt has the greatest effect of all the phases studied on the diffusion coefficients of the surface Cl^-, as expected from its large permanent positive structural charge. The diffusion coefficients of the inner-sphere complexes are reduced by a factor of about 14 relative to those of the bulk solution, and that of the outer-sphere complexes is reduced by about a factor of 3. On average, surface-bound Cl^- ions are about an order of magnitude less mobile than chloride ions in a bulk solution. Friedel's salt develops its permanent positive charge by isomorphous substitution of Al for Ca in one-third of the octahedral sites in the hydroxide layers, with this substitution compensated by anions (Cl^- in our case) in the interlayer space and on the surface.[27,35] Thus, some (run 3) or all (run 2) of the Cl^- ions in the simulations of it were originally part of the bulk structure. In contrast, in the portlandite simulations all of the surface anions and cations were originally part of the solution. Because of the positive charge on Friedel's salt, its surface density of Cl^- ions is significantly higher than that for portlandite (ca. 1.6 Cl^-/nm^2 vs 0.2 Cl^-/nm^2; see below).

Because of the difference in size between Ca and Al atoms that form the hydroxide layers of Friedel's salt, Ca atoms are displaced ~0.6 Å from the middle of their hydroxide layers along the *c*-direction, with half of them shifted up and half shifted down (Figure 2b and c). These structural arrangements produce two different types of positively charged sites on the basal surface of Friedel's salt to which Cl^- or H_2O molecules can coordinate. (Water molecules bear a negative partial charge on their O atoms and behave in many ways like the anions.) One of these types (Figure 2b) is similar to those on portlandite. It is located above Ca atoms shifted down from the middle of the surface hydroxide layer (away from the solution interface) and is formed by the hydroxyl groups bending toward the sorbed species. All sites of this type are occupied by Cl^- anions in the ordered interlayer structure of Friedel's salt.[35] In the interlayer, each of them is coordinated by three OH groups from the "upper" hydroxide layer, three OH

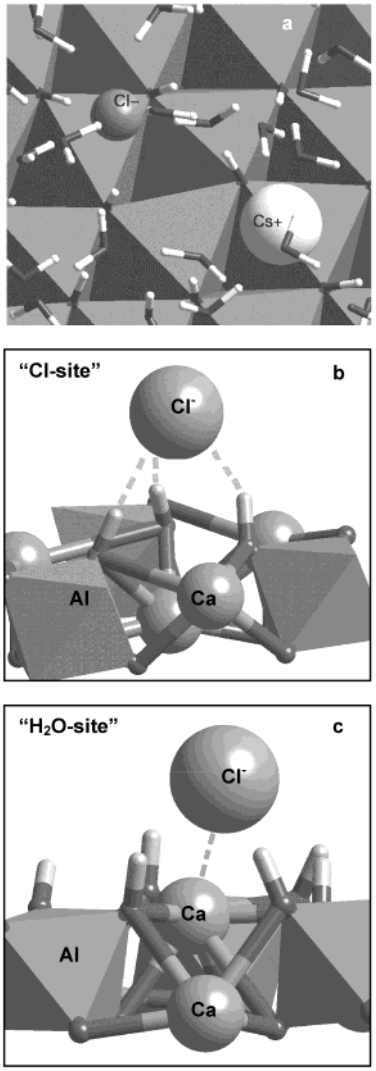

Figure 2. Portions of the simulated interfaces illustrating local surface bonding environments. See text for details. (a) Cs^+ and Cl^- on portlandite illustrating the importance of the flexibility of the surface OH groups. Surface OH groups and H_2O molecules in solution are shown as sticks and arrow-shaped objects, respectively. (b) The "Cl-type" adsorption site on the surface of Friedel's salt. Hydration water molecules are hidden for clarity. (c) The "H_2O-type" adsorption site on the surface of Friedel's salt. Hydration water molecules are hidden for clarity.

groups from the "lower" hydroxide layer, and four hydrogens of neighboring H_2O molecules (all through H-bonds). This symmetric H-bonding arrangement keeps interlayer Cl^- ions virtually immobile even at high temperatures.[27] Indeed, we observe no statistically appreciable Cl^- diffusion in the Friedel's salt interlayer ($D \ll 10^{-7}$ cm^2/s; Table 4). This diffusion coefficient is known experimentally to be about 10^{-8} cm^2/s.[43]

The second type of positively charged surface site on Friedel's salt is located directly above the Ca ions that are displaced about 0.6 Å from the middle of surface hydroxide toward the solution interface.[27,35] In the fully ordered interlayer, all sites of this type are occupied by water molecules, completing the unusual 7-fold coordination of each Ca atom in this structure. In MD simulations, the mobility of Cl^- ions adsorbed as inner-sphere complexes on this type of site (Figure 2c) is about a factor of 2 less than that for those sorbed at regular Cl^- sites (Figure 2b). This is presumably due to a higher Coulombic attraction to the Ca^{2+}.

Movement of ions among inner-sphere, outer-sphere, and bulk environments is clearly observable on the time scale of our simulations. Approximate Cl^- residence times on the inner-sphere surface sites are about 20 ps for portlandite and 50 ps for Friedel's salt and ettringite (Table 3), although the statistical uncertainty of these values is large because of the small number of ions in the simulations. The lower value for portlandite is consistent with its lack of permanent structural charge. These residence times are also consistent with the rapid hopping of Cl^- between surface and solution-like sites ($\tau < 10^{-6}$ s) observed for pastes of Friedel's salt and water using ^{35}Cl NMR spectroscopy.[44]

Dynamics of Surface Species. Spectra of atomic motions in the translational, librational, and vibrational frequency ranges allow comprehensive and detailed analysis of the dynamics of surface species, and their comparison to the dynamics of interlayer Cl^- in Friedel's salt[27] and in bulk solution. These power spectra are calculated from the simulated MD trajectories as Fourier transforms of the corresponding atomic velocity autocorrelation functions.[41] In the Friedel's salt interlayer, the spectral density of Cl^- translational motions (low-frequency vibrations) consists of two distinct bands centered at approximately 50 and 150 cm^{-1} (dashed line in Figure 3a). Decomposition of Cl^- velocities into components parallel and perpendicular to the layers indicates that the 50 cm^{-1} band is associated with "in-plane" motions and that the 150 cm^{-1} band is associated with vibrations perpendicular to the layers (insets in Figure 3a). Because each Cl^- is hydrogen-bonded to neighboring water molecules and OH groups, these two O···Cl···O modes are directly analogous to the intermolecular O···O···O bending and stretching motions of water molecules in H-bonded networks, respectively.[45−47]

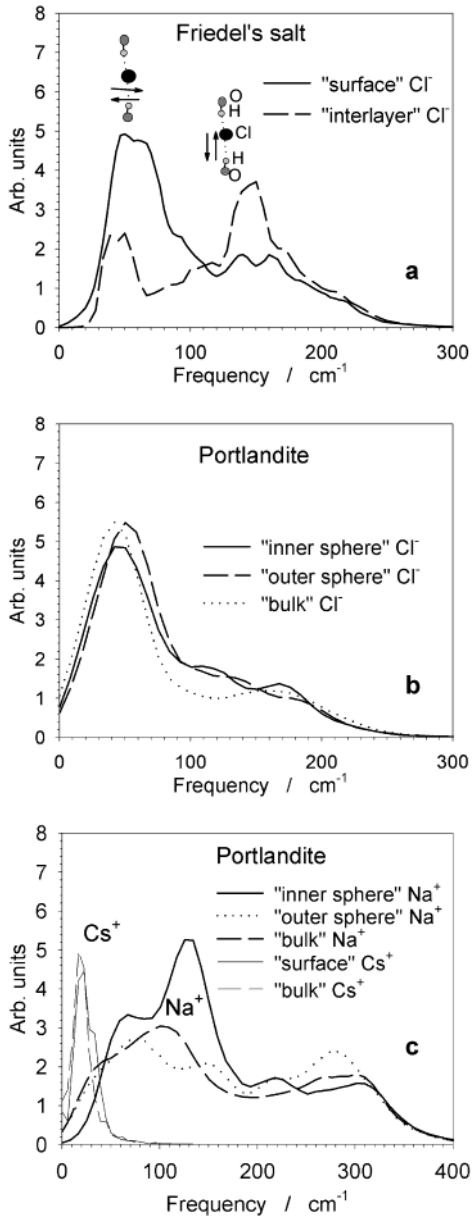

Figure 3. Spectral densities (power spectra) of low-frequency vibrational motions of adsorbed ions on the surface of Friedel's salt (a) and portlandite (b and c). Two characteristic modes of Cl^- dynamics are schematically shown as insets.

The power spectra of Cl^- on inner-sphere and outer-sphere surface sites of both Friedel's salt and portlandite resemble that of bulk aqueous Cl^- ions (dotted line in Figure 3b) more than that of interlayer Cl^-. The spectrum of inner-sphere Cl^- on Friedel's salt resembles that of interlayer Cl^- the most, and its band near 50 cm^{-1} is relatively narrow. The nearest neighbor structural environments of this type of surface site are more similar to those in the interlayer than the others. Similarly, the spectrum of outer-sphere Cl^- on portlandite most closely resembles that of a bulk solution. It is important to note that the similarity of Cl^- structural and dynamic behavior among interlayer, surface, and bulk hydrated environments is also observed for a variety of other hydroxide phases.[28−30]

The frequency range below ~50 cm^{-1} is especially important in this comparison, because the spectra of Cl^- on portlandite and in bulk solution have significant

(43) Buenfeld, N. R.; Zhang, J. Z. *Cem. Concr. Res.* **1998**, *28*, 665.
(44) Kirkpatrick, R. J.; Yu, P.; Hou, X.; Kim, Y. *Am. Mineral.* **1999**, *84*, 1186.
(45) Eisenberg, D.; Kauzmann, W. *The Structure and Properties of Water*; Oxford University Press: Oxford, 1969.
(46) Heinzinger, K. In *Computer modeling of fluids, polymers and solids*; Catlow, C. R. A., Ed.; Kluwer Academic Publishing: 1990; p 357.
(47) Kalinichev, A. G.; Heinzinger, K. *Adv. Phys. Geochem.* **1992**, *10*, 1.

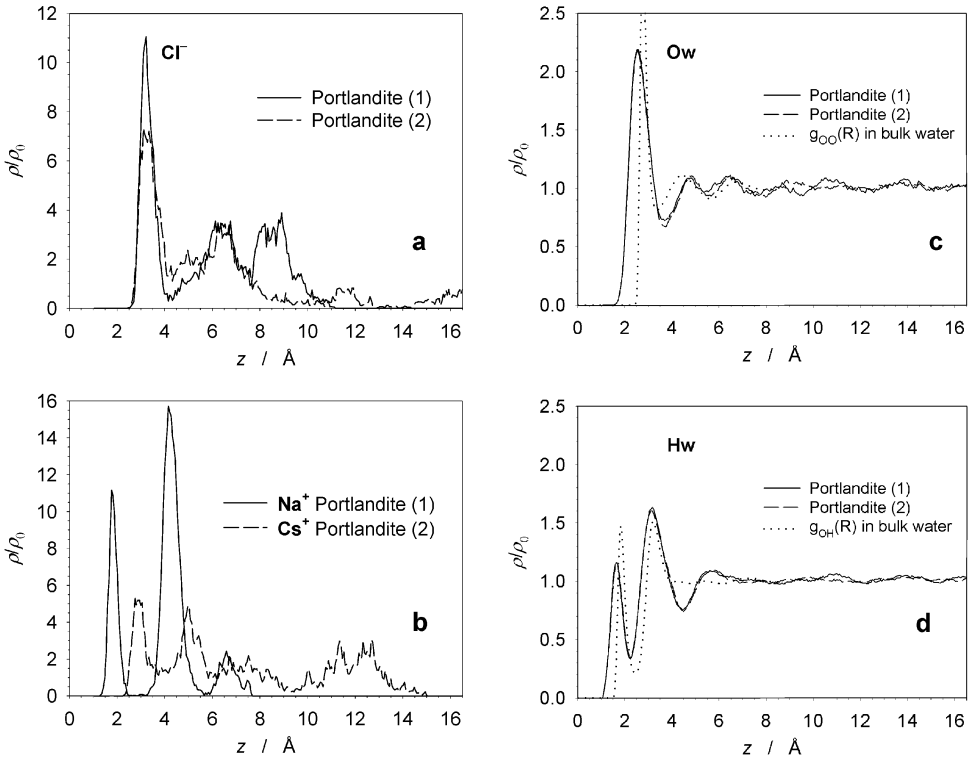

Figure 4. Density profiles of the indicated solution species at the surface of portlandite. Oxygen atoms of the closest to the solution hydroxide layer are located in the plane $z = 0$. The O−O and O−H radial distribution functions of bulk water are shown as dotted lines for comparison.

intensities at $\nu = 0$ for translational motions, whereas they are very low for Friedel's salt and especially for interlayer Cl^-. The zero-frequency value of the power spectrum is proportional to the self-diffusion coefficient of the molecules.[41] Our previous computational results for interlayer and surface H_2O and Cl^- in LDHs show that their mobility is indeed dramatically decreased relative to those typical for bulk solutions, despite the observed similarities in their local structural and dynamic environments. This result correlates well with the calculated diffusion coefficients for these different sites (Table 4). Additionally, the band near 150 cm^{-1} is less intense for the surface species than that in the Friedel's salt interlayer, probably because of the absence of a planar symmetry in the positive charge distribution on both sides of Cl^-.

The cations Na^+ and Cs^+ sorbed on portlandite behave quite differently (Figure 3c). For heavy and slow Cs^+ there is no statistically significant difference in the translational dynamics on surface sites and in bulk solution. In contrast, for smaller and faster Na^+, on inner-sphere sites there is increased prominence of a band near 140 cm^{-1}, and the dynamics of the adsorbed species is clearly distinguishable from that of bulk hydrated ions.

It is important to emphasize that the frequency range associated with the translational dynamics of surface-sorbed species discussed above (Figure 3) overlaps with the range characteristic of the numerous modes of low-frequency lattice vibrations of the metal hydroxide octahedra in the solid structure.[30,48] Thus, the dynamics of the surface species can be strongly coupled to these vibrational modes of the solid substrate. This can serve as an additional argument in favor of explicit treatment of the dynamics of substrate atoms in MD simulations of solid/solution interfaces.

Structure at the Interfaces. The structures of solutions at and near interfaces with solids are difficult to study and poorly known,[2] although new experimental methods based on the high-resolution X-ray reflectivity measurements of solid/water interfaces are recently beginning to emerge.[49] Computed atomic density distribution functions perpendicular to the solution/solid interface and in the plane of the interface are useful tools to quantitatively analyze this structure.[15,16,46,50] Such density profiles are similar to atomic radial distribution functions in bulk solutions, and can eventually be directly compared with experimentally determined electron density profiles across the interface, resulting from X-ray reflectivity measurements.[49] Here the calculated atomic density profiles are averaged over the two statistically equivalent interfaces of the simulated systems (e.g., Figure 1). For portlandite, the results of both MD runs show that on average ~1.5 Cl^- ions (out of 4 present in the solution) occur in inner-sphere coordination (0−4 Å from the surface) at any instant (Figure 4a), and ~1.2 Cl^- occur in outer-sphere coordination (4−8 Å from the surface). A total of ~65% of all chlorides in the solution are surface-bound (see also Table 3), and the surface density is ~0.2 ions/nm^2. The peak near 9 Å on the Cl^- density profile for run 1

(48) Ruan, H. D.; Frost, R. L.; Kloprogge, J. T.; Duong, L. *Spectrochim. Acta A* **2002**, *58*, 265.

(49) Cheng, L.; Fenter, P.; Nagy, K. L.; Schlegel, M. L.; Sturchio, N. C. *Phys. Rev. Lett.* **2001**, *8715*, 156103−1.

(50) Spohr, E. *Electrochim. Acta* **1999**, *44*, 1697.

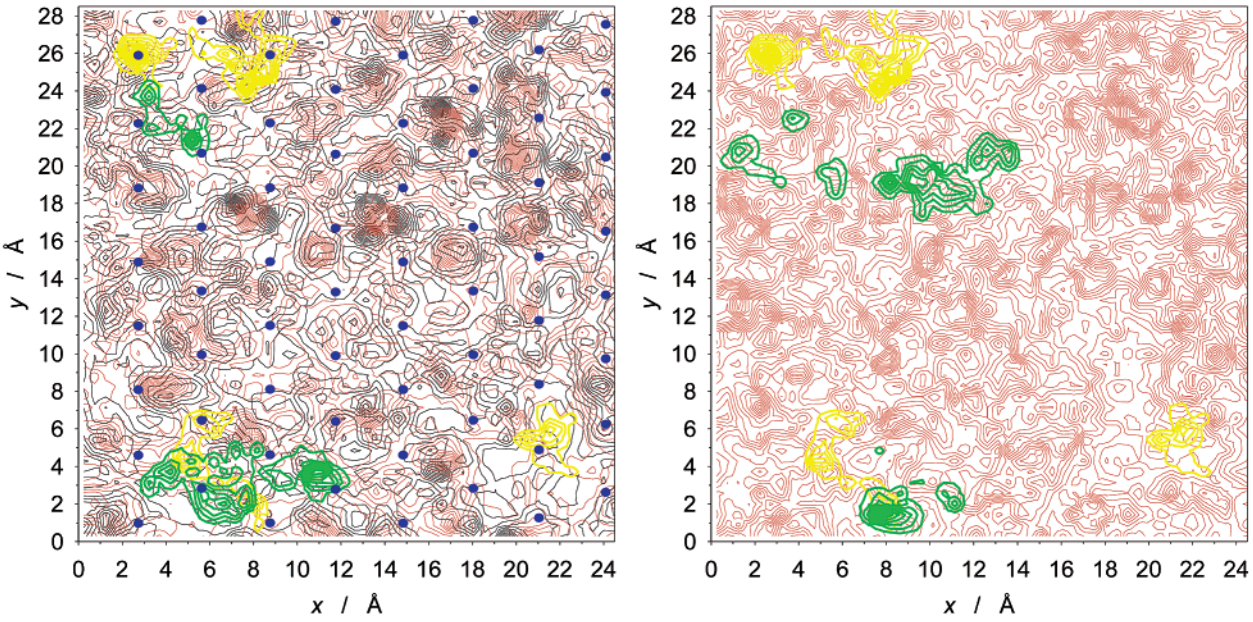

Figure 5. Contour maps of atomic density for solution species at the surface of portlandite (simulation run 2). Left: 0−4 Å solution layer representing inner-sphere coordination. Right: 4−8 Å solution layer representing outer-sphere coordination. Blue dots are the positions of Ca atoms in the underlying hydroxide layer; green contours are for surface Cl^- ions; yellow contours are for surface Cs^+ ions; red contours are for O atoms of H_2O molecules; and black contours are for H atoms of H_2O molecules.

(Figure 4a) is due to a relatively stable Na^+-Cl^- ion pair formed in the bulk solution during the simulation (see also the Na^+ peak at ∼7 Å in Figure 4b).

For all density profiles, the origin ($z = 0$) of the surface is defined as the average position of the layer where surface oxygens of the solid atoms (here, OH groups) are located. Thus, the absolute positions of, for example, inner-sphere and outer-sphere atoms reflect the atomic radii of the species. Well-defined inner-sphere and outer-sphere complexes are also present for the cations on portlandite (Figure 4b). A relatively larger fraction of surface-associated Na^+ occurs in outer-sphere coordination, and approximately ∼85% of all Na^+ ions are surface-bound (inner-sphere or outer-sphere), as opposed to only ∼60% for Cs^+.

Time-averaged contour maps of atomic densities for slices different distances from the surface (e.g., Figure 5 for portlandite) provide useful visual insight into the sites occupied by surface species, their vertical and horizontal mobility, and the spatial relationships among atoms in the solution (e.g., ion pair formation). To increase visual contrast in these diagrams, we have normalized the atomic density distributions for each species to the respective maximum values for that particular species. Comparison of the inner-sphere (0−4 Å) and outer-sphere (4−8 Å) slices for portlandite (Figure 5) illustrates the movement of the 2 Cl^- and 2 Cs^+ ions on this particular surface between different positions in the same layer and between inner-sphere and outer-sphere sites. They also indicate the existence of a strong spatial correlation between adsorbed Cl^- and Cs^+ ions and, thus, the formation of relatively stable ion pairs on the surface. Similar behavior is also observed for portlandite with NaCl solution (run 1). Yu and Kirkpatrick[10,11] have suggested that the formation of ion clusters can significantly increase the extent of Cl^- sorption on portlandite, and the MD simulations here are consistent with this proposal.

The computed atomic density profiles also provide important insight into the ordering of water molecules at the interface. Two orientations of H_2O molecules are energetically most favorable for the formation of stable hydrogen bonds to the calcium hydroxide surface. In one of them, water molecules have one H atom directed toward an O atom of the surface hydroxyl, thus donating a hydrogen bond to the surface. This is reflected in the presence of a strong peak at ∼1.8 Å on the H_w density profile (Figure 4d). In this orientation, the second H atom contributes to the peak at ∼3.2 Å. However, a stronger contribution to the 3.2 Å peak in the H_w distribution arises from the other favorable H_2O orientation, in which O atoms of water molecules accept hydrogen bonds donated by the surface hydroxyl groups. In this case, both hydrogens of the H_2O molecule contribute to the density profile peak at 3.2 Å. Such surface sites are comparable to those occupied by Cl^- (Figure 2). In both preferred orientations of H_2O molecules, the O atoms are located approximately the same distance from the surface (∼3.0 Å) and only slightly closer than Cl^- (Figure 4a). The ability of the surface water molecules to both donate and accept hydrogen bonds to and from the solid surface creates a very well-developed hydrogen-bonding network across the interface with the structure strongly resembling that of bulk liquid water. O−O and O−H radial distribution functions of liquid water are shown as dotted lines in Figure 4c and d to illustrate this similarity. The interface water is slightly more structured than bulk H_2O under the same thermodynamic conditions,[26] and this ordering of the water molecules is clearly visible even at distances up to 8 Å from the surface (red contours in Figure 5).

For Friedel's salt (runs 3 and 4) the computed near-surface solution structure is strikingly different. Because of the positive structural charge of this phase and the possibility of direct coordination of surface Ca sites by water molecules[27] or Cl^- ions (Figure 2c), the H-bond

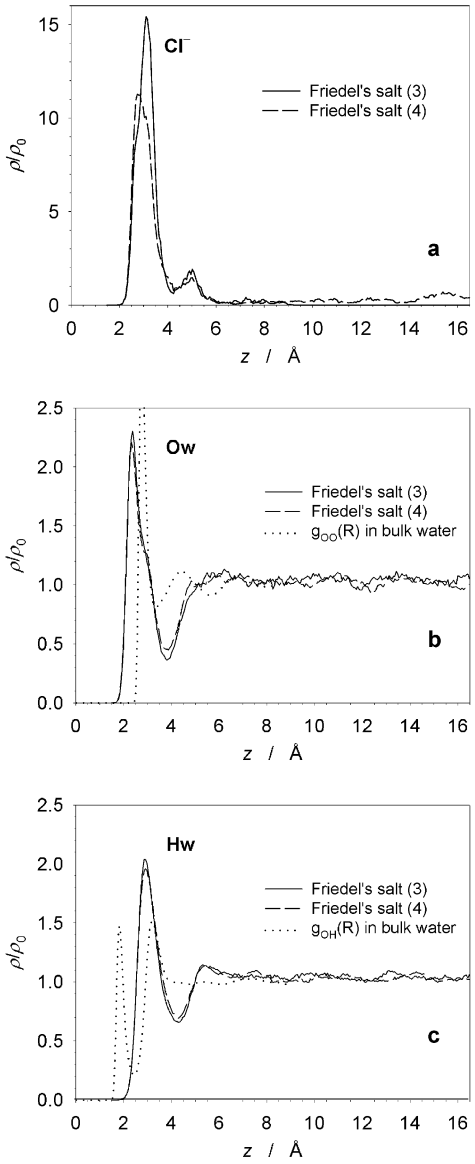

Figure 6. Density profiles for the indicated solution species at the surface of Friedel's salt. Oxygen atoms of the closest to the solution hydroxide layer are located in the plane $z = 0$. The O−O and O−H radial distribution functions of bulk water are shown as dotted lines for comparison.

donation to the surface by H_2O molecules is prevented and the well-interconnected H-bonding network is not formed in the interfacial region of the Ca_2Al double hydroxide (Figures 6 and 7). The presence of two preferred types of surface adsorption sites for Cl^- and H_2O (Figure 2b and c) is reflected in slightly split peaks for inner-sphere Cl^- and H_2O in the density profiles (Figure 6a and b). Despite slightly different distributions of adsorbed Cl^- between the two types of inner-sphere sites in the two different simulations (peaks near 3 Å in Figure 6a), both runs gave essentially identical overall results with ~13.5 Cl^- in inner-sphere coordination, ~1.7 Cl^- in outer-sphere coordination, and a total surface density of ~1.6 Cl^-/nm^2. No Na^+ ions were observed at distances less than 8 Å from the surface in run 4, where it was present.

The contour maps of atomic densities for Friedel's salt (Figure 7) show a high degree of Cl^- and H_2O ordering at distances 0−4 Å from the surface (inner-sphere coordination), with up to half of all Cl^- ions occupying the "H_2O sites" (indicated as blue dots in Figure 7; see also Figure 2c). However, in contrast to the case for the portlandite surface, none of the surface O atoms of Friedel's salt are able to serve as an acceptor of H-bonds from water molecules in the aqueous phase, and the charged solid surface dominates the interfacial solution structure, rather than a well-developed network of hydrogen bonds. Thus, the short-range structure of the solution interface is strikingly different from that of bulk water (dotted lines in Figure 6b and c), and there is no significant water structuring beyond ~5 Å from the surface. While the tetrahedral near-neighbor ordering of the H-bonding networks (reflected in the second peak of O−O radial distribution functions of water at ~4.5 Å)[26,45−47] is well-maintained for the partlandite/water interface (Figure 4c), it is completely destroyed at the interface with Friedel's salt (Figure 6b). This destructive effect of the charged surface on the hydrogen-bonding in the interfacial solution is comparable to the effects of high temperature, high pressure, and highly charged dissolved species on the structure of bulk water.[26,47]

Conclusions

Using a recently developed force field, we have successfully simulated the structures of portlandite, Friedel's salt, tobermorite, ettringite, and their interfaces with aqueous chloride solutions using molecular dynamics methods. For the first time, the atomistic mechanisms of chloride binding to cement phases have been studied on a fundamental molecular scale. The MD simulations demonstrate the importance of taking into account the mobility and flexibility of the surface OH groups for realistic modeling of local electrostatic environments favorable for adsorption of cations and anions on hydroxides. The dynamics of the translational motions (low-frequency vibrations) of Cl^- absorbed on the surfaces of portlandite and Friedel's salt is dominated by two distinct bands centered at approximately 50 and 150 cm^{-1} and corresponding to bending and stretching of hydrogen bonds formed among the anions, surface hydroxyls, and neighboring water molecules. A very well-developed H-bonding network is formed across the interface of the aqueous phase in contact with calcium hydroxide, whereas the formation of such a tetrahedrally ordered network of H-bonds is prevented in the interfacial region of the Ca_2Al double hydroxide (Friedel's salt) because of the polarizing effect of its structural charge. The chloride-binding capacity observed in the MD simulations decreases in the sequence Friedel's salt > portlandite > ettringite > tobermorite, which is in excellent agreement with recent experimental sorption and ^{35}Cl NMR studies.[10,11]

The principal limitation of the molecular modeling approach is the accuracy of the interatomic potentials applied in the simulations.[18,26] The CLAYFF force field[19] used here was not specifically optimized to reproduce the structure and dynamics of the materials and surface species discussed in this paper. However, good agreement of the simulated properties with available experimental data for the systems discussed here and elsewhere[29,30] demonstrates great robustness of the CLAYFF force field and its significant potential in helping to understand the details of the structural and dynamic

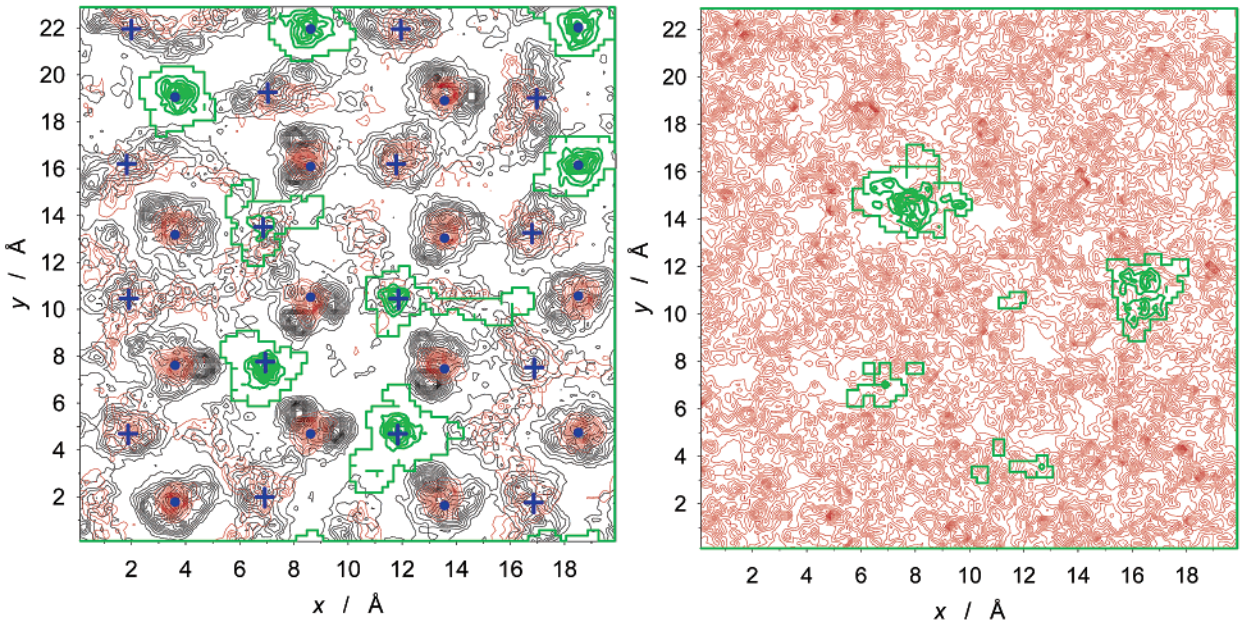

Figure 7. Contour maps of atomic density for solution species at the surface of Friedel's salt (simulation run 3). Left: 0−4 Å solution layer representing inner-sphere coordination. Right: 4−8 Å solution layer representing outer-sphere coordination. Blue dots and crosses are the positions of Ca atoms in the underlying hydroxide layer ("H_2O-sites" and "Cl-sites", respectively; see also Figure 2b and c). Green contours are surface Cl^- ions; red contours are O atoms of H_2O molecules; black contours are H atoms of H_2O molecules.

behavior of aqueous species in confined environments dominated by hydrogen-bonding and electrostatic interactions, such as hydrated surfaces of clay, cement, metal hydroxide, and LDH phases, as well as other materials often characterized by complex, disordered, and ill-defined structure and composition.

Acknowledgment. The research was supported by the DOE (Grant DEF02-00ER1528), by the NSF (Grant EAR 97-05746), and by industrial funding to the Center for Advanced Cement-Based Materials. The computations were supported by the National Computational Science Alliance (Grant EAR 990003N), and utilized NCSA SGI/CRAY Origin2000 computers and the Cerius^2-4.0 software package from Molecular Simulations Inc. The collaboration with Dr. R. T. Cygan in the development of the force field parameters for the simulations is most gratefully acknowledged.

Supporting Information Available: The full set of force field parameters used, and full-color snapshots of representative portions of the simulated structures of Friedel's salt, tobermorite, and ettringite (PDF). This material is available free of charge via the Internet at http://pubs.acs.org.

CM0107070

Table 1s. Force filed parameters of the simulation model. [a]

	σ_{ii} / Å	ε_{ii} / kJ/mol	q_i / e
Oxide / hydroxide structure			
Ca	5.56	2.10×10^{-5}	1.05
Al	4.27	5.56×10^{-6}	1.575
O (portlandite)	3.166	0.650	–0.95
O (Friedel's salt)	3.166	0.650	–0.87083
O (ettringite)	3.166	0.650	–0.8675
O1 (tobermorite)	3.166	0.650	–1.1305
O2 (tobermorite)	3.166	0.650	–1.0808
H (hydroxide)	—	—	0.425
Interlayer and aqueous species			
O (water) [b]	3.166	0.650	–0.82
H (water) [b]	—	—	+0.41
Cl^- [c]	4.401	0.418	–1.0
Na^+ [c]	2.584	0.418	+1.0
K^+ [c]	3.332	0.418	+1.0
Cs^+ [c]	3.884	0.418	+1.0
S (SO_4) [d]	3.55	1.046	+2.0
O (SO_4) [d]	3.15	0.837	–1.0

[a] Cygan, R. T.; Liang, J.; Kalinichev, A. G. *J. Phys. Chem. B* **2002**, submitted.

[b] Berendsen, H.J.C. et al. *In: Intermolecular Forces*; Pullman, B., ed., Riedel, Dordrecht, **1981**, p.331.

[c] Dang, L. X. *J. Am. Chem. Soc.* **1995**, *117*, 6954.

[d] Cannon, W. R.; Pettitt, B. M.; McCammon J. A. *J. Phys. Chem.* **1994**, *98*, 6225.

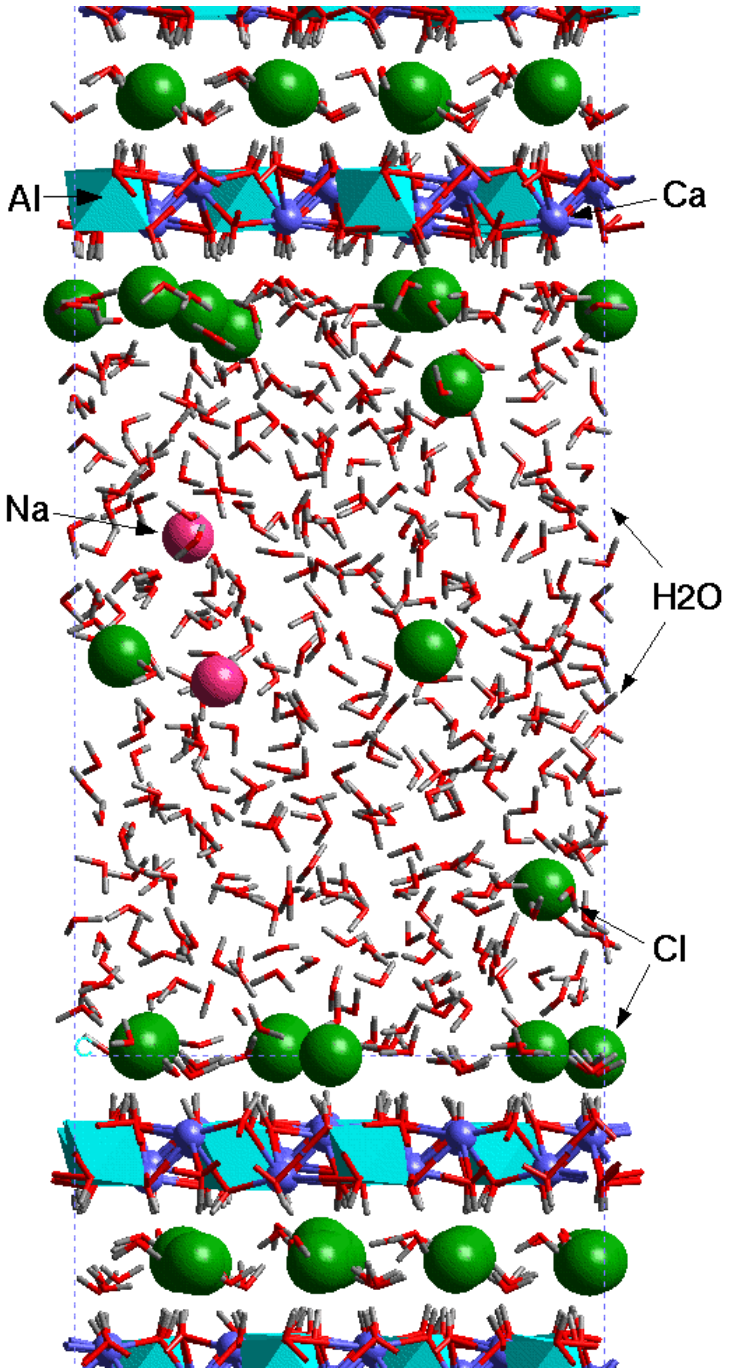

Fig. 1s. A simulation snapshot of the Friedel's salt, $[Ca_2Al(OH)_6]Cl{\cdot}2H_2O$, interface with 0.28*m* NaCl aqueous solution. Dark blue balls – Ca; light blue octahedra – Al; red cylinders – O; gray cylinders – H; green balls – Cl ions; pink balls – Na ions. Only parts of the solid layer are shown above and below the solution layer.

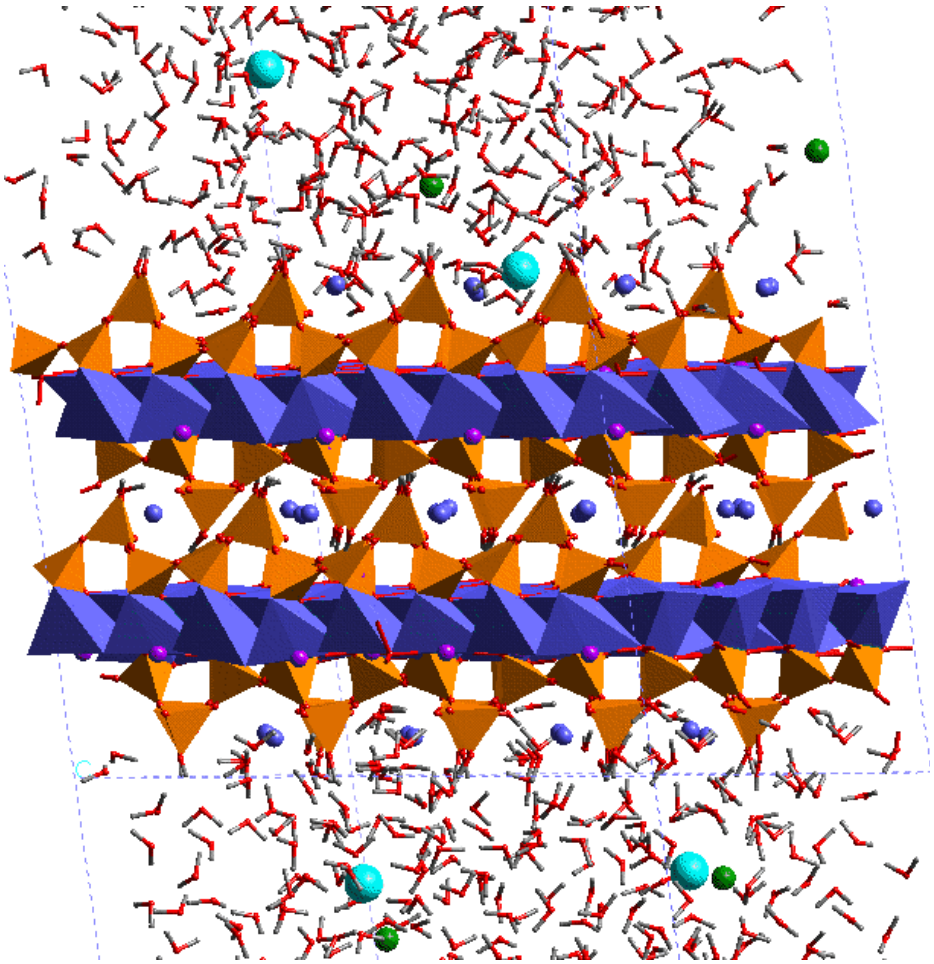

Fig. 2s. A simulation snapshot of the tobermorite, $Ca_5Si_6O_{16}(OH)_2$, interface with 0.25*m* KCl aqueous solution. Dark blue balls and octahedra – Ca atoms in two different structural positions within the "tobermorite 9 Å" structure (Merlino et al., 1999); orange tetrahedra – Si; red cylinders – O; gray cylinders – H; green balls – Cl ions; light blue balls – K ions. Only parts of the solution layer close to the interface are shown above and below the solid layer.

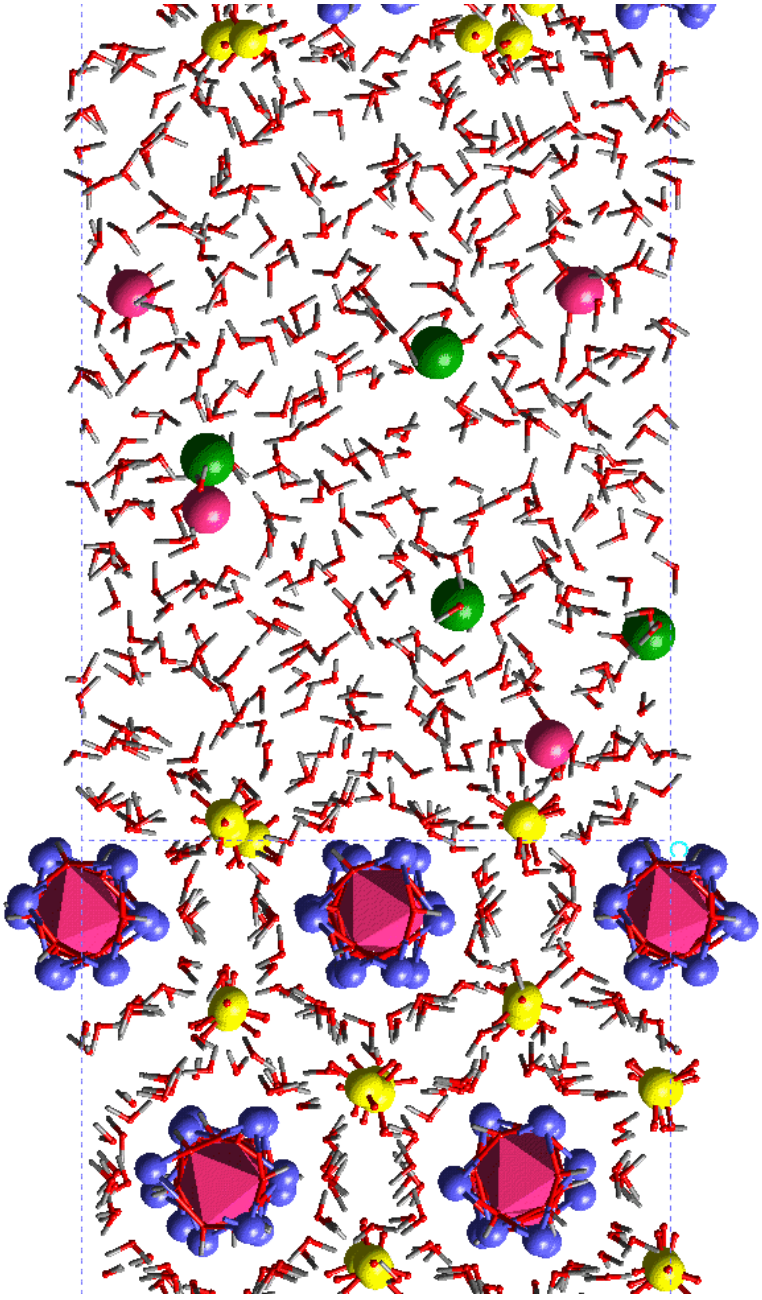

Fig. 3s. A simulation snapshot of the ettringite, $Ca_6[Al(OH)_6]_2[SO_4]_3 \cdot 26H_2O$, interface with 0.4*m* NaCl aqueous solution. Dark blue balls – Ca; pink octahedra – Al; red cylinders – O; gray cylinders – H; green balls – Cl ions; pink balls – Na ions; yellow balls – S of sulfate ions. Only parts of the solid layer are shown above and below the solution layer.